

AUTHOR QUERY FORM

 ELSEVIER	Journal: FOOHYD Article Number: 4426	Please e-mail your responses and any corrections to: E-mail: corrections.esch@elsevier.tnq.co.in
--	---	--

Dear Author,

Please check your proof carefully and mark all corrections at the appropriate place in the proof (e.g., by using on-screen annotation in the PDF file) or compile them in a separate list. **It is crucial that you NOT make direct edits to the PDF using the editing tools as doing so could lead us to overlook your desired changes.** Note: if you opt to annotate the file with software other than Adobe Reader then please also highlight the appropriate place in the PDF file. To ensure fast publication of your paper please return your corrections within 48 hours.

For correction or revision of any artwork, please consult <http://www.elsevier.com/artworkinstructions>.

Any queries or remarks that have arisen during the processing of your manuscript are listed below and highlighted by flags in the proof.

Location in article	Query / Remark: Click on the Q link to find the query's location in text Please insert your reply or correction at the corresponding line in the proof
Q1	Please confirm that the provided email(s) nhm443@bham.ac.uk is/are the correct address for official communication, else provide an alternate e-mail address to replace the existing one, because private e-mail addresses should not be used in articles as the address for communication.
Q2	The citation 'Li & Nie, 2016' has been changed to match the author name in the reference list. Please check here and in subsequent occurrences, and correct if necessary.
Q3	The following citations "Nussinovitch 2007" are unlisted.
Q4	Please provide the volume number or issue number or page range or article number for the bibliography in Ref(s). Nishino et al., 2011.
Q5	Please note that as per the journal style, if there are more than 6 authors/editors, the first 6 author names are listed followed by 'et al.' if the author group consists of 6 authors or fewer, all author names should be listed. Therefore, in Ref(s). Arvanitoyannis et al, 1993; Asami et al, 2003; Barresi et al, 2009; Capek et al, 2010; Gormley et al, 2002; Harnkarnsujarit et al, 2016; Huang et al, 2009; Kravtchenko et al, 1999; Moreno et al, 2015; Nakagawa et al, 2006; Nowak et al, 2016; Patel et al, 2017; Rambhatla et al, 2004; Saifullah et al, 2016; Sangamithra et al, 2015; Silva et al, 2015; Voda et al, 2012; Xu et al, 2006; Zea et al, 2013; please list all names for up to 6 authors/editors. For more than 6 authors/editors, use 'et al.' after the first 6 authors/editors.
Q6	Uncited references: This section comprises references that occur in the reference list but not in the body of the text. Please position each reference in the text or, alternatively, delete it. Any reference not dealt with will be retained in this section. Thank you.
Q7	Please confirm that given names and surnames have been identified correctly and are presented in the desired order and please carefully verify the spelling of all authors' names.

(continued on next page)

Q8

Your article is registered as a regular item and is being processed for inclusion in a regular issue of the journal. If this is NOT correct and your article belongs to a Special Issue/Collection please contact t.sivakumar@elsevier.com immediately prior to returning your corrections.

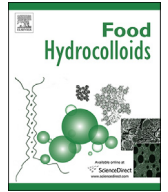
Please check this box or indicate
your approval if you have no
corrections to make to the PDF file

Thank you for your assistance.



Contents lists available at ScienceDirect

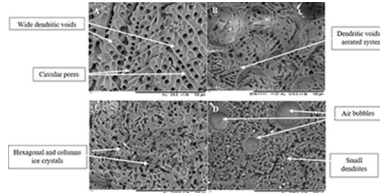
Food Hydrocolloids

journal homepage: www.elsevier.com/locate/foodhyd

Graphical Abstract

Effect of freezing on microstructure and reconstitution of freeze-dried high solid hydrocolloid-based systems

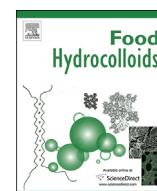
pp. 1–12

N. Malik^a, O. Gouseti, S. Bakalis



Contents lists available at ScienceDirect

Food Hydrocolloids

journal homepage: www.elsevier.com/locate/foodhyd

Effect of freezing on microstructure and reconstitution of freeze-dried high solid hydrocolloid-based systems

N. Malik^{a,*}, O. Gouseti^b, S. Bakalis^b^a School of Chemical Engineering, University of Birmingham, B15 2TT, UK^b The University of Nottingham, NG7 2RD, UK

ARTICLE INFO

Article history:

Received 1 March 2018

Received in revised form

4 May 2018

Accepted 6 May 2018

Available online xxx

Keywords:

Freeze-drying

Freezing

Hydrocolloids

Concentrated systems

Ice crystals morphology

Microstructure

ABSTRACT

Freeze-drying has been associated with high quality hydrocolloid-based products such as coffee. However, it is an expensive technique, and one way to reduce energy and water use is by drying concentrated systems. Controlling the ice crystal formation is important to produce final dried materials with desired microstructure and properties. This study presents the effect of freezing with and without temperature oscillations on the final microstructure and reconstitution of aerated and non-aerated freeze-dried concentrated (50 and 60% w/w) gum arabic and coffee systems. Samples were either frozen at -40°C or subjected to fluctuating temperatures between -40 and -20°C prior to drying. Thermal analysis of the systems showed lower nucleation and freezing temperatures for 50% compared to 60% solutions, as expected, and melting temperatures $> -20^{\circ}\text{C}$. During drying, puffing of the material was observed, with appearance of a glass-like, puffed bottom layer, in particular for the 60% coffee frozen at -40°C . SEM micrographs revealed pores of dendritic, hexagonal, and circular shape, indicating voids produced by sublimation of ice crystals. Pore sizes were smaller (by 50%, of the order of 40nm) for the 60%, than the 50% systems. Temperature fluctuations during freezing doubled the observed pore sizes and the apparent total porosity which effectively accelerated the dissolution kinetics. Aeration resulted in the appearance of air bubbles (diameter $200\text{--}1600\text{ }\mu\text{m}$) that largely phase separated in gum arabic and resulted in faster rehydrating solids. This work demonstrates the potential of process design to control microstructural attributes and reconstitution properties of freeze-dried hydrocolloid-based products in systems with high solute concentrations.

© 2018 Published by Elsevier Ltd.

1. Introduction

The highly branched structure of polysaccharides known as hydrocolloids are mainly associated with the ability to modify viscosity of food products. Presence of the colloidal particles such as galactomannans and arabinogalactans in food formulations like sauces, ice-cream, salad dressings and coffee created end product with characteristic texture and sensory properties (Li & Nie, 2016). For example, the creamy sensation and foaming ability of coffee solutions has been linked with these high molecular weight polysaccharides in the coffee extract (Nunes & Coimbra, 2002). Meanwhile, the arabinogalactoprotein fraction in gum arabic made it widely used as emulsifier (Nishino, Katayama, Sakata, Al-Assaf, &

Philip, 2011). Drying of hydrocolloid-based systems is important for food applications to produce materials with the desired characteristics, such as texture, shelf life, or rehydration capacity (Cassanelli, Norton, & Mills, 2017). Dried hydrocolloid systems have also applications in other sectors, including medicine (Nussinovitch, Velez-Silvestre, & Peleg, 1993) and pharmaceuticals (Gal & Nussinovitch 2007; Mukai-Correa et al., 2004). In foods, quality of dried products is usually characterized by flavour, aroma and nutrients retention as well as porosity and reconstitution properties.

Freeze-drying is one of the most preferred drying techniques for quality products such as instant coffee, partially because of its ability to yield highly porous microstructures that contribute to high rehydration capacity of the freeze-dried foods (Ishwarya & Anandharamakrishnan, 2015; Asami et al., 2003). In freeze-drying, food is initially frozen to induce water crystallisation and it is subsequently dehydrated through sublimation of the ice and desorption of the unfrozen water. The freezing step is critical as the

* Corresponding author. Department of Chemical Engineering, University of Birmingham, Edgbaston, B15 2TT, UK.

E-mail address: nhm443@bham.ac.uk (N. Malik).

morphology of the ice crystals formed determine the final morphology of the freeze-dried cake and hence the properties of the dehydrated product.

Freezing involves ice nucleation and crystal growth. In concentrated systems, freezing of water is limited by the reduced water availability, due to the low water content, and lower molecular mobility, due to the high viscosity. The possibility to control ice crystals' size and shape through modification of the freezing process has been previously discussed (Kiani & Sun, 2011). This includes utilisation of emerging techniques, such as ultrasonic vibration, which has been shown to promote growth of large and directional dendrites due to nucleation induced at high temperature (Nakagawa et al., 2006). Other ways to control water crystallisation include addition of nucleating agents such as *Pseudomonas Syringae* and silver iodide (AgI) (Searles, Carpenter, & Randolph, 2001), freezing with nitrogen gas (Rambhatla et al., 2004), and annealing (Hottot, Vessot, & Andrieu, 2007). These techniques were introduced to have ice nucleated at the desired temperature and eventually growth of the desired ice crystal morphology. Annealing is carried out at the end of the freezing process by holding the sample above the glass transition temperature, and below melting, for a certain period of time. This holding step allows growth of large crystals, assisted by the recrystallisation phenomenon known as Ostwald ripening (Hottot et al., 2007).

Ice crystals may also play a critical role in the dehydration step, where it is important that sufficient heat and mass transfer occur during drying for efficient process. For example, small crystals have been correlated with high vapour flow resistance and low drying rate (Ceballos, Giraldo, & Orrego, 2012; Harnkarnsujarit, Charoenrein, & Roos, 2012; Searles, 2010). The high resistance at the sublimation front can cause overheating to the product due to prolonged exposure in the drying stage (Franks, 1998). A danger of overheating means there is possibility for product temperature to reach higher than its glass transition (T_g) or collapse temperature (T_c) leading to increased molecular mobility and eventually structural collapse (Krokida, Karathanos, & Maroulis, 1998; Levi & Karel, 1995; Overcashier, Patapoff, & Hsu, 1999; Tsourouflis, Flink, & Karel, 1976). Knowledge of glass transition, collapse temperature (T_c) and melting temperature (T_m) of food materials is important for the choice of the most appropriate processing parameters (Roos, 1997). A collapsed freeze-dried cake is often associated with dense structure (Krokida et al., 1998) and poor rehydration capacity (Barresi et al., 2009).

Numerous work have shown how attributes of freeze-dried foods are controlled by the freezing conditions applied (Ceballos et al., 2012; Hottot, Vessot, & Andrieu, 2004a; Liliiana, Diana, & Alfredo, 2015; Nowak et al., 2016; Voda et al., 2012). However, understanding the link between freezing conditions and properties of the dried materials is still a matter of on-going research. For example, during rapid freezing to temperatures $< -80^\circ\text{C}$, formation of needle-like ice crystals and eventually narrow voids has been reported, and it was linked with instantaneous rehydration of the freeze-dried protein based food and carrot (Harnkarnsujarit et al., 2016; Voda et al., 2012). On the contrary, Ceballos et al. (2012) reported that solubility of freeze-dried fruit powders decreased with increasing freezing rate due to high capillary resistance in small pores. Large crystals formation due to slow freezing has been further linked with good water uptake during rehydration in freeze-dried starch-based foods (Koh, Rhim, & Kim, 2011). These studies highlight the importance of controlling ice crystal formation to ensure desired quality characteristics of the final dried product.

Freeze-drying demands significant energy consumption and investigations to minimise time and energy usage during processing have been carried out in the past decades (Huang et al., 2009;

Patel, Doen, & Pikal, 2010). Operational models taking into account different heat and mass transfer principles as well as materials formulations have been proposed for a simple and convenient tool to optimise processing and minimise the energy consumption and, thereby, facilitate the process design of freeze-drying technology (Liu, Zhao, & Feng, 2008; Luo & Zhou, 2008). Determining the point in which sublimation ends has been suggested by Patel et al. (2010) to be useful for optimisation of the primary drying step. The author evaluated different methods to determine the end point of freeze drying such as comparative pressure measurement, measuring water concentration and product temperature. The contributions of different investigations showed that drying pre-treatments including microwave and osmotic dehydration, increased the energy saving during freeze-drying (Huang et al., 2009; Liapis & Bruttini, 2008; Pardo & Leiva, 2010; Xu et al., 2006). Foaming or aeration as pre-treatments has also been proposed to increase drying rate and improve process economics for example, freeze-drying of foamed apple juice and egg white showed positive impact on reducing the total drying time (Muthukumaran, Ratti, & Raghavan, 2008; Raharitsifa & Ratti, 2010). The porous nature and larger surface area of foamed materials has been identified to shorten the drying time, which lowers the energy expenditure (Kudra & Ratti, 2006; Sangamithra et al., 2015).

In this study, processing of high solids system is considered as a means to lower the energy impact during processing due to the small fraction of water involved. However, ice crystal development during the freezing stage constitutes a challenge for low moisture food systems due to reduced water availability and molecular mobility. To address the process-structure-quality relationship in freeze-dried high solid systems, the effect of aeration as pre-treatment as well as freezing with temperature oscillation on the final microstructure and dissolution behavior of freeze-dried concentrated solutions (50 and 60% by weight) were studied. Gum arabic and coffee were used as a model and real food systems, respectively. Both samples are rich in arabinogalactans responsible for the distinctive texture and sensory properties of hydrocolloids based food formulations (Capek et al., 2010; Gashua, Williams, & Baldwin, 2016). Freeze-dried samples were observed using scanning electron microscopy (SEM) and image analysis was applied to characterise the microstructural attributes. Dissolution behavior of the freeze-dried solids was determined to correlate microstructure with its rehydration properties.

2. Materials and methods

2.1. Sample preparation

Gum arabic powder (Sigma-Aldrich Co. Germany) and freeze-dried coffee granules (purchased from local store) were used in this work. These materials were selected as they are both rich in arabinogalactan, arabinogalactan-protein complex and glycoprotein. For sample preparation, the required amount of solid material was weighed and dissolved in distilled water under heating (45–50 °C) with mixing at 250 rpm using hot plate to prepare solutions of 50 and 60% w/w solute. Solutions were then degassed to remove excess air bubbles incorporated during dissolution. Coffee samples were degassed using ultrasonic cleaning bath with de-gas function (USC 300 THD-45 Hz, Leicestershire, UK) while air bubbles in the gum arabic systems were removed manually after overnight gravimetric separation at room temperature (20 °C). Aerated systems were further prepared by incorporating 30–40% of air into the degassed system using domestic food processor (Kenwood 300 Watt-CH180A, Hampshire, UK). The required amount of air was added to achieve density of 0.8gcm^{-3} and 1.2gcm^{-3} for the coffee and gum arabic systems, respectively.

2.2. Freezing and freeze-drying

28 mL of each prepared solutions were transferred into aluminium trays (internal diameter of 85 mm, height 20 mm) and were subsequently placed onto the shelf of the freeze-drier (VirTis AdVantage Plus 2.0 Benchtop shelf based freeze-dryer, SP Industries, Warminster, PA, USA). The investigated freezing and freeze-drying conditions are schematically shown in Fig. 1. For freezing, shelf temperature was set to decrease from 20 °C to -40 °C at 1 °C/min and it was then either kept at 40 °C for 6 h or it was set to fluctuate between -40 °C and -20 °C for 4 h holding at each temperature for 30 min, followed by 2 h tempering at -40 °C. Sample temperature during freezing was monitored using K-type temperature sensor probes, which were carefully positioned at the middle of the tray. Triplicate samples were used and nucleation temperature as well as freezing time was derived from the cooling curves.

2.3. Differential scanning calorimetry (DSC)

State and phase transitions of the (degassed) systems were analysed with a differential scanning calorimeter (DSC, Mettler Toledo 821e with liquid N₂ cooling, Leicester, UK). Samples (7–18 mg) were placed on a pre-weighed 40 µl DSC aluminium pans (Mettler Toledo, Leicester, UK) and hermetically sealed. The samples and a reference pan containing air were transferred to the DSC device and cooled and scanned from 20 °C to -80 °C at 1 °C/min, then held at -80 °C for 5 min and finally heated to 20 °C using the same rate. Meanwhile, thermal profile of 60% gum arabic was obtained by scanning from 50 °C to -80 °C. The higher temperature was applied because crystallisation peak for this system could be observed when scanned from lower temperature. Duplicate samples were used and the average onset crystallisation and melting temperatures were determined from the thermal profile recorded.

2.4. Structure analysis

Obtained freeze-dried cakes were fractured carefully lengthwise by hand and cross-sections were photographed using a digital single-lens reflex camera (Canon DSLR EOS 5D Mark II, Middlesex, UK). A section from the middle of the cake representative of the cake's morphology alongside its height was further analysed with X-Ray Computer Tomography (Skyscan 1172, Bruker MicroCT, Kontich, Belgium) under medium camera setting (2000 × 1048 pixels) with X-ray source set to 50–70 kV (100 µA). Before scanning,

the cut sample was carefully mounted on a sample holder equipped with blue tac to prevent the sample from moving while rotating. The distance between X-ray source, object and camera was adjusted to produce 8 µm pixel images. Three frame averaging, rotation step of 0.40° and exposure time between 200 and 300 ms were chosen to minimise the noise, covering a view of 180°. A typical scan took around 25–30 min. NRecon software package (Bruker MicroCT) was then used for reconstruction of the 2D cross-section images. Representative cross-section images were converted to binary images by thresholding using CTAn software package (Bruker MicroCT).

Microstructure was examined in more detail with a Hitachi TM3030 Desktop SEM Microscope (Krefeld, Germany) operating with energy dispersive X-ray (EDX). Samples (5 mm × 10 mm) were fixed to an aluminium stub using double-sided carbon tape before being transferred to the SEM chamber. Images were collected under low vacuum (100 Pa) using energy dispersive X-ray (EDX) mode at 500× magnification.

Collected SEM images from triplicate experimental runs were analysed using ImageJ. An example of image analysis is shown in Fig. 2. Grayscale images were converted to binary images by thresholding and they were cleaned with despeckle filter function. An average of at least 300 pores from SEM cross-sections were selected for pore size determination. Similar images were then used for quantification of total porosity defined as the ration of pore area to the total area of image. In samples with large air bubbles, these were manually excluded in the estimation of pore sizes and included in the estimation of total porosity.

2.5. Reconstitution of freeze-dried sample

Reconstitution of dehydrated samples from temperature oscillation experiment were recorded with the inverted light microscope (Zeiss Axio vert.A1, Jena, Germany). Individual particles of each sample (freeze-dried coffee and gum arabic) was prepared by cutting into approximately 0.5 mm². Each particle was placed in a 294 mm³ glass petri dish which contains 10 ml distilled water at room temperature. Image resolution was set as 1376 × 1038 pixels and images were recorded at 5 frames per second by the open source software µManager. To enhance the contrast of the image a black and a white hardboard was put underneath the glass petri dish during the reconstitution of gum arabic and freeze dried coffee respectively.

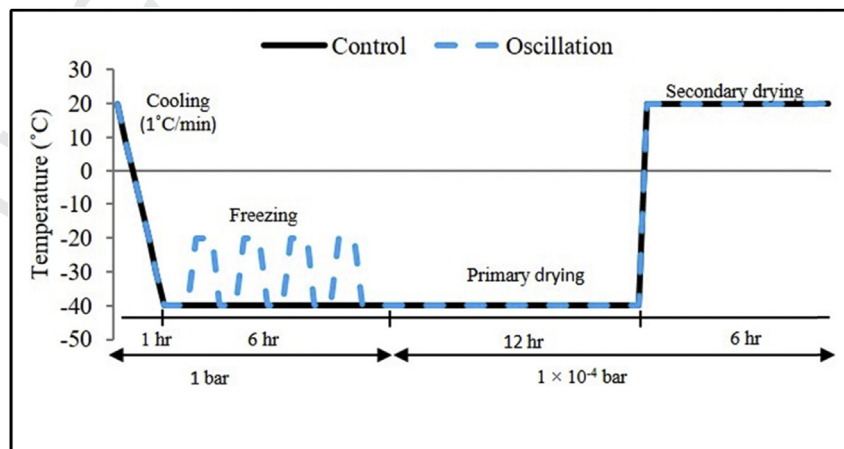


Fig. 1. Time and temperature profile of freeze-drying cycles.

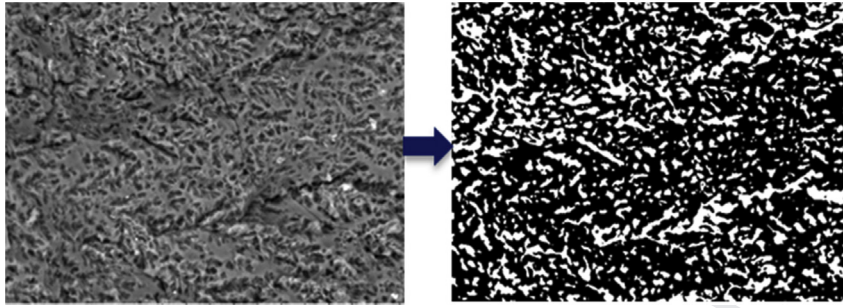


Fig. 2. Schematic representation of image processing.

2.6. Statistical analysis

Analyses were carried out in triplicate and error bars represent plus/minus a single standard deviation.

3. Results and discussion

Results are presented in three sections. Thermal properties are presented first, followed by a discussion on the observed structures of the freeze-dried solids and finally their reconstitution properties.

3.1. Thermal properties

Two methods were used to study thermal properties: DSC (degassed systems only) and temperature recording (TR) during freezing (all systems). The DSC curves were analysed to determine the onset freezing (T_{F-DSC}) and onset melting (T_m) of the materials, and results shown in Table 1. TR curves (Fig. 3) had shapes typical of freezing curves, showing nucleation and freezing regimes, and were analysed to determine nucleation (T_n) and freezing (T_{F-TR}) temperatures (data shown in Table 2). T_n and T_{F-TR} were determined as the lowest temperature reached during supercooling and the peak temperature reached during crystallisation, respectively (as also shown in the capture of Fig. 3a). The peak of supercooling was difficult to detect for the 60% initial concentration systems, in particular the degassed gum arabic solution. It is noted that T_n and T_{F-DSC} signify the beginning of crystallisation, while T_{F-TR} and T_m are indicative of the thermodynamic transition temperature.

Tables 1 and 2 indicate that freezing, melting, and nucleation temperatures decreased (by 44% on average) on increase of concentration (from 50 to 60%). This trend has previously been attributed to lower water availability as well as reduced mobility of the water molecules, associated with increased viscosity, at higher solid contents (Arvanitoyannis et al., 1993; Homer, Kelly, & Day, 2014). For 60% concentrations, comparable onset melting temperatures to those of Table 1 (which also correspond to T_{F-TR} of Table 2) have been reported for sucrose (Roos & Karel, 1991), fructose (Ablett et al., 1993), and starch (Homer et al., 2014). Unlike concentration, aeration appeared to have marginal effect on nucleation and freezing temperatures (see Fig. 3 and Table 2).

Coffee showed overall lower transition temperatures than gum

arabic. This is indicative of a less thermodynamically stable system and may be attributed to the different molecular organisations and interactions occurring in the two materials due to their non-identical composition (Rahman, 2006). In this study, T_{F-TR} recorded for coffee solutions were lower than values reported by Burmester, Fehr, and Eggers (2011) but comparable with Moreno et al. (2015). Burmester et al. (2011) reported T_f at $-6 \pm 6^\circ\text{C}$ and $-12 \pm 6^\circ\text{C}$ for coffee solutions with 50% and 60% solid while the latter study identified T_f at $-9.8 \pm 0.24^\circ\text{C}$ for the 50% concentration.

It should be noted that although the above trends were evident in both DSC and TR data, comparing the onset of freezing (from Table 1) with the nucleation temperature (from Table 2), which both signify the beginning of crystallisation, indicates that DSC produced lower (by approximately 10°C) values than the thermocouple recording method. The difference between the two techniques may be linked to the different cooling rates exerted on the sample: $1^\circ\text{C}/\text{min}$ for DSC and $2.5^\circ\text{C}/\text{min}$ for freezing in the freeze-drier (determined from the TR freezing curves).

3.2. Morphology

Morphology of the dried materials was examined at macroscopic scale (cross-sections of the dried cakes) with high-resolution camera (photos of Fig. 4) and X-Ray CT analysis (Fig. 5), as well as at microscopic scale with SEM (Figs. 6–7).

3.3. Macroscopic structure

Fig. 4 indicates that formulation and freezing conditions both affected the appearance of the dried cakes. For example, freeze-drying of aerated systems resulted in cakes with overall uniform appearance, whereas formation of two distinctive top and bottom layers was observed in dried degassed systems, in particular at higher initial solid content. In these cases, the top crusts had macroscopic structures similar to those of the uniformly dried aerated systems with no signs of melting or collapse. The bottom layers were darker and glass-like, suggesting that the material melted and re-solidified during drying. This indicates that in these parts, the sample's local temperature exceeded the melting temperature, despite the freeze-dryer shelf temperature (at -40°C) being lower than T_m (see Table 1). The most affected morphologies were those of the degassed 60% initial concentration coffee and, to a lesser extent, gum arabic frozen at -40°C prior to drying (Fig. 4i and k). Application of freezing cycles increased the thickness of the top dried layer (Fig. 4m and °, respectively).

Structural changes during freeze-drying have been extensively studied in the context of pharmaceutical formulations and are typically associated with structure collapse and volume reduction (Patel et al., 2017). In the present work, X-Ray CT images (Fig. 5)

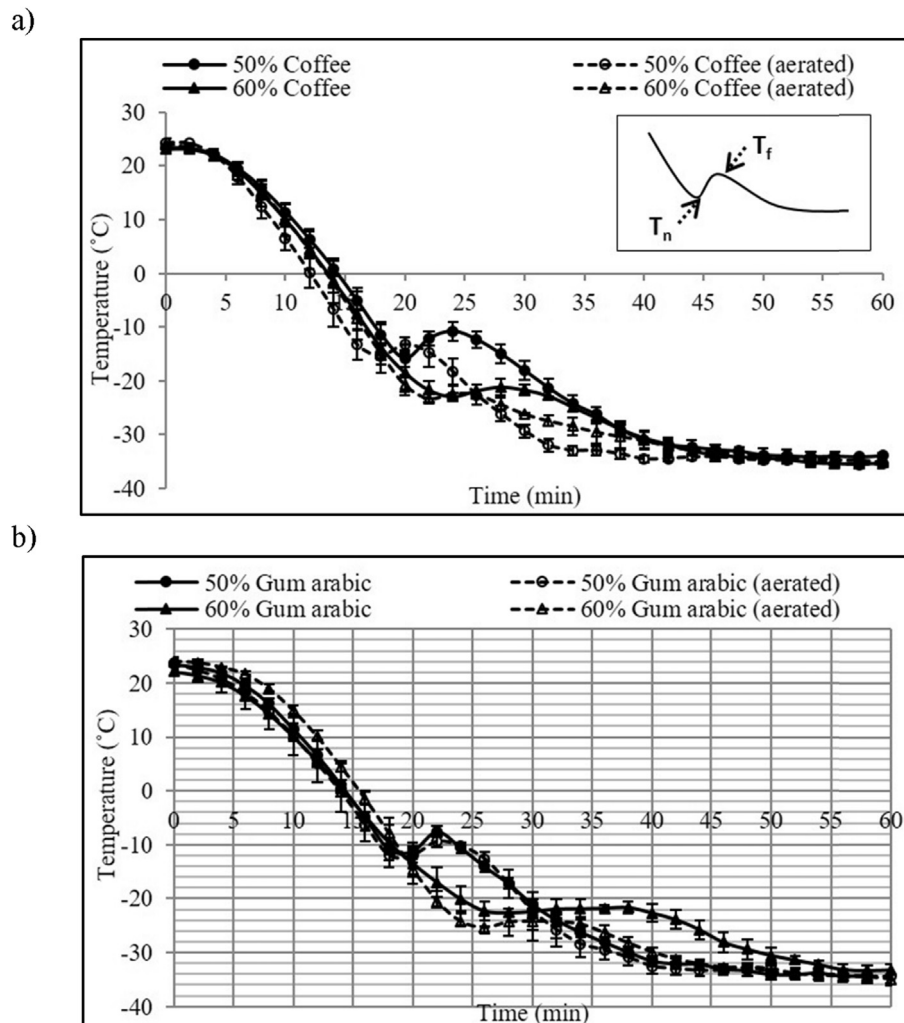


Fig. 3. Cooling curves of (a) coffee and (b) gum arabic systems during freezing to -40°C .

Table 2

Freezing properties of concentrated food systems determined using thermocouples to measure the temperature during freezing (T_n : nucleation temperature, T_{f-TR} : freezing temperature).

System	50% coffee		60% coffee		50% gum arabic		60% gum arabic	
	No air	Aerated	No air	Aerated	No air	Aerated	No air	Aerated
T_n ($^{\circ}\text{C}$)	-16 ± 2	-15 ± 1	-23 ± 1	-23 ± 1	-11 ± 1	-12 ± 1	–	-25 ± 0
T_{f-TR} ($^{\circ}\text{C}$)	-11 ± 2	-13 ± 2	-22 ± 4	-23 ± 3	-8 ± 2	-10 ± 1	-23 ± 2	-25 ± 2

indicate formation of large pores of circular-type cross-sections in the bottom layers. These highly porous structures suggest that the material in the present work puffed during drying rather than collapsed. Puffing suggests that there is internal pressure build-up in the drying material that exceeds the strength of its surrounding causing the observed expansion. It is possible that as drying progresses from top to bottom, the rapidly frozen top crust may obstruct the vapour pathway and therefore vapour from the sublimated water is entrapped in the bottom layer. As drying continues, additional vapour is accumulated to the bottom layer increasing the inner pressure of the system and also the inner temperature (through the produced latent heat). This may cause melting of the ice, if sample temperature exceeds melting temperature. The inner pressure build-up, combined with the melted, mobile surroundings and the low pressure (vacuum) of the freeze-

dryer may further cause formation of the observed large pores. Inner structure expansion may also be partially responsible for cracking of the top crust, which is evident in Fig. 5. As the bottom layer expanded, cracking of the top layer may have occurred, allowing the release of entrapped vapour from the bottom layer out of the sample. The cracked structure might further be the result of pressure build-up during secondary drying. At this stage, unfrozen water is evaporated from the dried solids at high temperature (20°C) that can impart stress. Thus, cracks begin to develop allowing evaporated liquid being removed. Cracking in freeze-drying have been identified in a recent evaluation as a response to the increasing stress during evaporation of unfrozen liquid (Patel et al., 2017; Ullrich, Seyferth, & Lee, 2015).

It is expected that systems with higher initial solid content (i.e. 60% compared to 50%) will experience higher degree of melting/

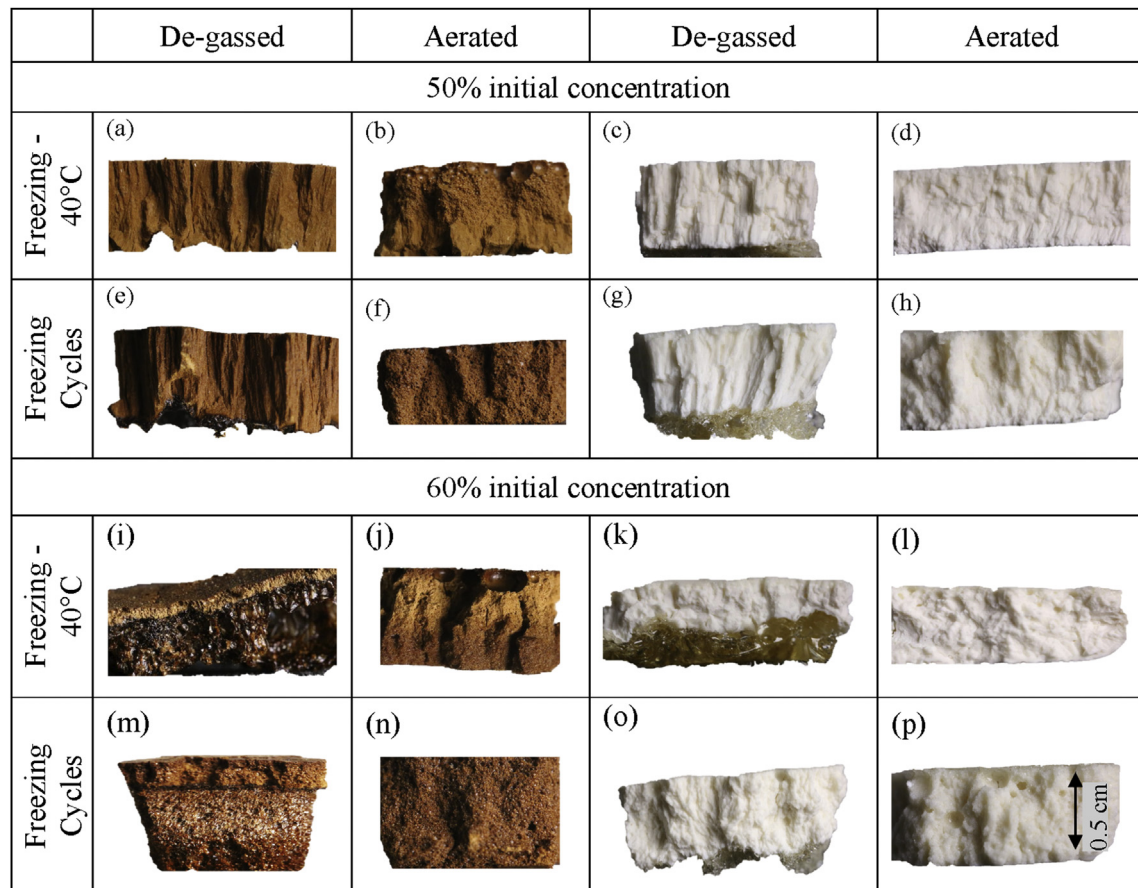


Fig. 4. High-resolution images of freeze-dried cakes' cross-sections.

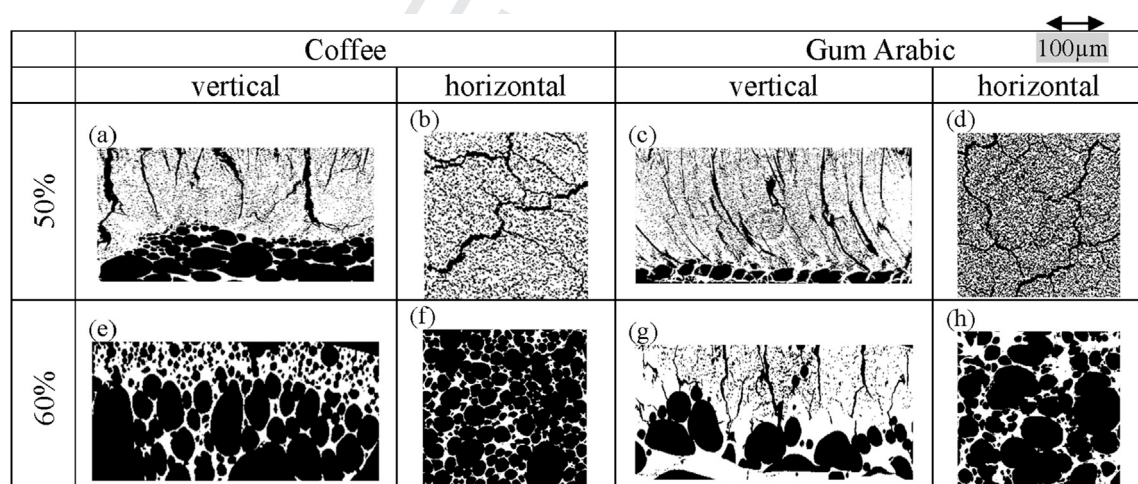


Fig. 5. X-Ray CT images of the freeze-dried cakes' cross sections in height (a, c, e, g) and radially (b, d, f, h).

puffing through (i) reduced porosity in the top crust as there is less ice to sublimate (evident also in the SEM images, see Fig. 6); and (ii) reduced T_m (see Table 1) that is easier to overcome. Application of freezing cycles, similarly to annealing, resulted in the formation of larger ice crystals that during drying provide a dried top crust with larger pores that may allow escape of the produced vapour as freeze-drying progresses. This results in the observed structures with thicker top dried layers and less evident melting appearance

(Fig. 4). Aeration prior to freezing and freeze-drying produced structures with high uniformity, indicating that mass and heat transfer through the dried layer was enough to avoid vapour entrapment in the structure.

3.4. Microscopic structure

The top layers were further analysed with SEM to examine their

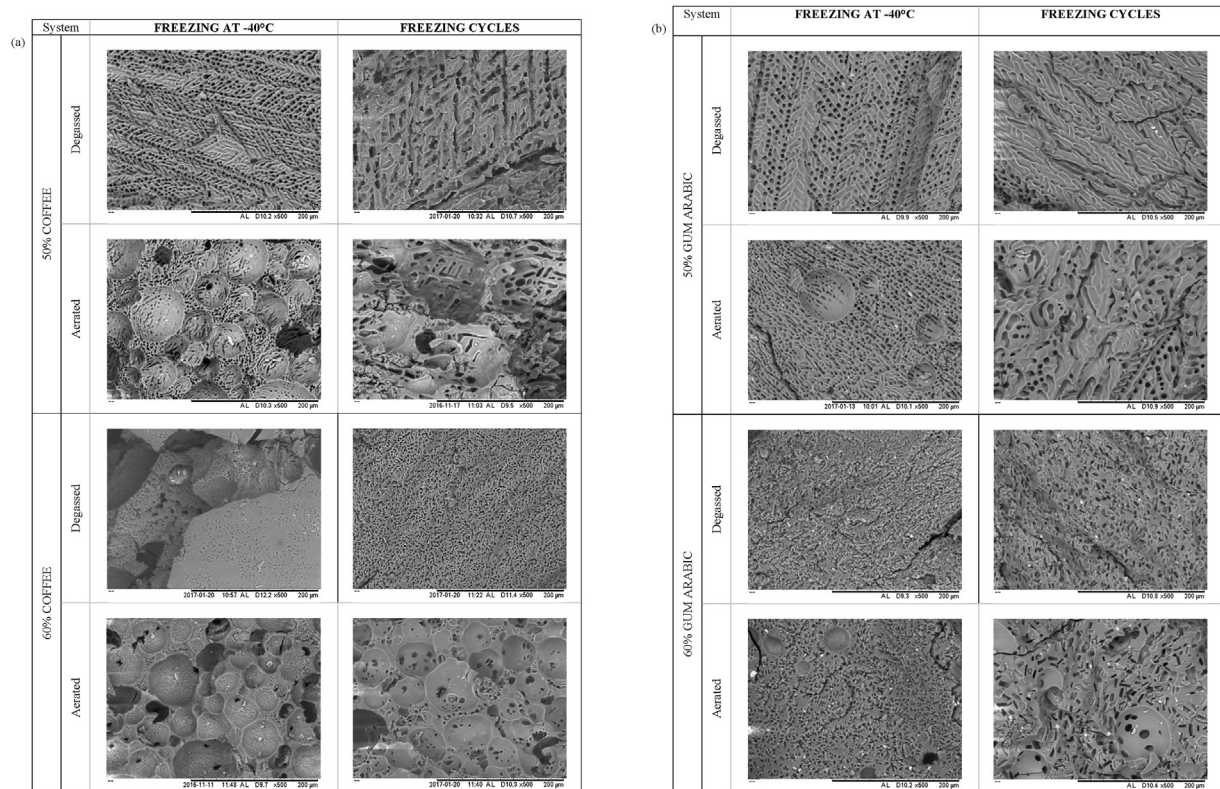


Fig. 6. SEM images of investigated (a) coffee and (b) gum arabic systems (bar is 200 µm).

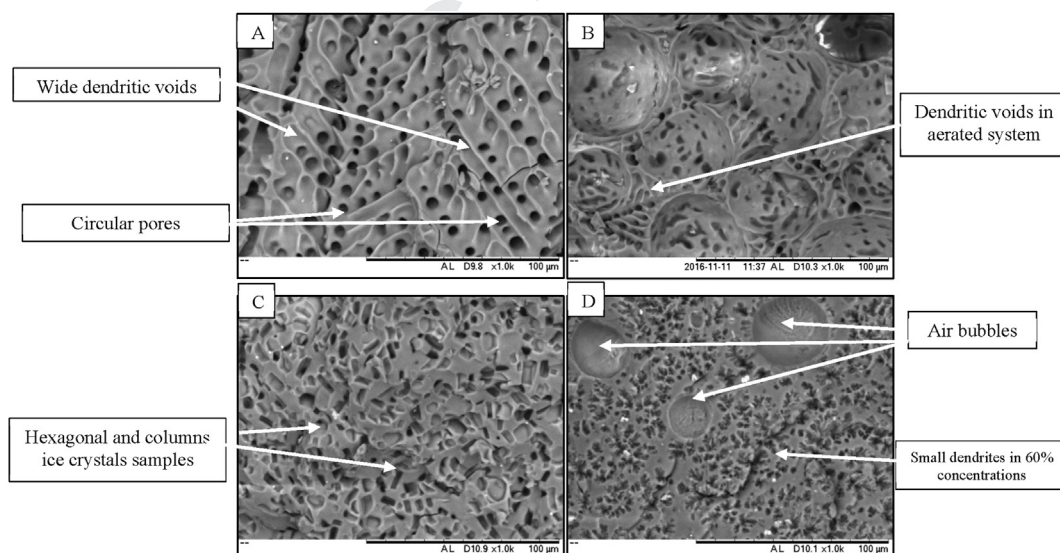


Fig. 7. Different ice crystals and pores morphology observed in SEM micrographs at 1000x of freeze-dried matrices.

internal structures, and representative images at two magnifications are shown in Fig. 6 (lower magnification) and 7 (higher magnification). Overall porous structures were observed with two sets of pores: those with sizes of the order of 100 µm, and those with circular cross-sections and sizes of the order of 0.5–1 mm or higher. These large pores were evident principally in aerated systems and are attributed to air bubbles created during aeration of the systems. In the case of the degassed 60% coffee frozen at -40°C , sampling from the thin top crust was difficult and large pores have

been associated with air bubbles created during expansion of the bottom layers, as discussed previously (see Figs. 4 and 5). Small pores are attributed to voids created after sublimation of ice. They have dendritic (see Figs. 6 and 7) and hexagonal (see Fig. 7) shapes, typical of ice crystals found in frozen foods (Petzold & Aguilera, 2009). Small circular and rectangular pores were also observed (see Figs. 6 and 7), and these are thought to be part of the dendritic network and the hexagonal ice, respectively, seen from different angles. Ignoring the large air bubbles, average diameters of circles

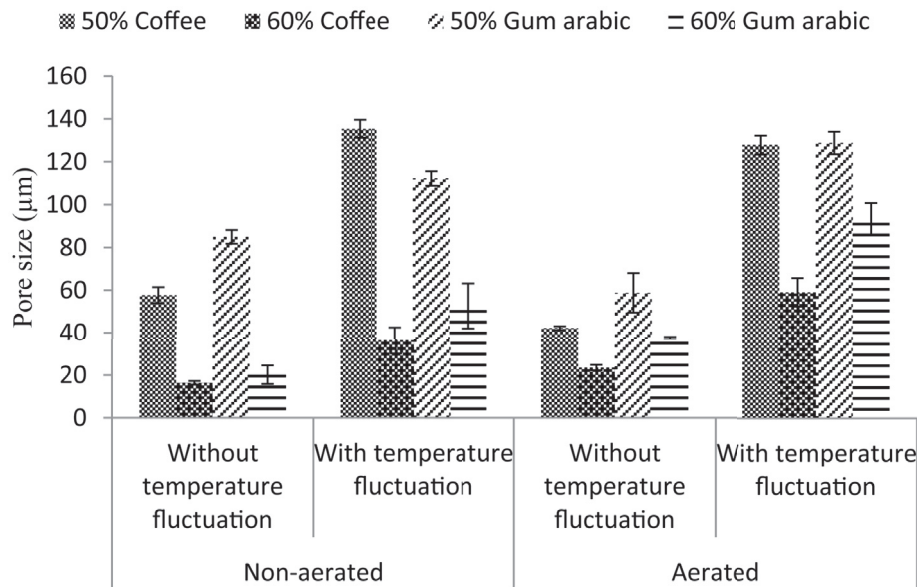


Fig. 8. Mean size of pores from ice crystals in freeze-dried samples frozen under various conditions.

having equal area as the obtained small pores are shown in Fig. 8.

Increasing concentration resulted in pore size reduction, indicating smaller ice crystal formation during freezing, which has previously been reported (see for example Pardo, Suess, & Niranjan, 2002). Dendritic voids with distinct directionality and sizes of 60–135 µm were observed for the 50% systems, and they were accompanied with small circular pores. Directionality may be attributed to the cooling direction, as samples were cooled from the bottom of the cake that was in contact with the frozen shelf, to the top that was exposed to the freeze-drying chamber. Meanwhile, freeze-drying the 60% solutions gave solids with much narrower dendrites, within the range of 20–30 µm area-equivalent circular diameter and absence of evident circular pores, indicating small dendritic networks.

Larger pores were displayed by samples freeze-dried with temperature oscillations, indicating larger ice crystal formation. This observation could be the result of sample being held at temperature above T_g and below T_m during the freezing step as this temperature range has been associated with higher crystallisation (Roos, 1997). Temperature fluctuations during freezing have similar effects as annealing, which promotes large ice crystals formation (Gormley et al., 2002; Kasper & Friess, 2011, pp. 248–263). Large ice crystals have also been linked with reduced freeze-drying times (Hottot, Vessot, & Andrieu, 2004b; Searles, 2010) attributed to the decrease in vapour flow resistance during drying due to the high porosity of the dried layer.

Inclusion of air generally showed marginal effect on the crystal formation. It appears that at 50% solids, aeration resulted in somehow smaller ice crystal formation, while the opposite effect was seen at 60% concentration (see Fig. 8). In addition, the surfaces

of air bubbles often appeared free of pores, particularly in 60% gum arabic system frozen without temperature oscillations. This may indicate that on those occasions air bubbles' surfaces acted as a barrier to crystal growth.

Air bubble distribution was different in the two aerated materials studied. Aerated coffee showed higher structural stability during freeze-drying and appearance of air bubbles was evident. Aerated gum arabic appeared to hold substantially less air within the cake structure after freeze-drying (see Fig. 6). Visual inspection of the cakes indicated that the air in the gum arabic systems was partially separated to the top of the cake (also seen with a careful look in Fig. 4). It is possible that this phase separation happened during freezing, as the air travelled upwards primarily due to density difference between the air and the solidifying liquid (assuming that the viscosity was low enough to allow the movement) and/or further aided by the changes that occurred in the system due to water crystallisation.

Diameter of air bubbles for each sample was estimated from 50 air bubbles due to limited number developed in gum arabic. On the contrary to mean pore sizes, size of air bubbles was not affected by concentration. Coffee had air bubbles with diameters of about 600 µm, whereas gum arabic displayed smaller diameters, around 400 µm. Temperature oscillation during freezing resulted in larger air bubbles (600–1600 µm diameter) in the freeze-dried material, more evenly distributed to the cake's body (see Fig. 6).

3.5. Porosity

Porosities of the freeze-dried solids were determined using two techniques. Firstly, binary SEM micrographs (see example of Fig. 2)

Table 3
Porosity (%) of the freeze-dried solids determined through image analysis.

System	Degassed		Aerated	
	Freezing -40°C	Freezing cycles	Freezing -40°C	Freezing cycles
50% Coffee	49 ± 2.81	58 ± 3.55	71 ± 1.56	75 ± 4.25
60% Coffee	28 ± 5.93	28 ± 1.67	65 ± 0.51	72 ± 0.57
50% Gum arabic	67 ± 2.89	78 ± 2.01	45 ± 0.72	73 ± 2.01
60% Gum arabic	35 ± 2.67	39 ± 1.23	34 ± 2.02	53 ± 3.67

Table 4
Porosity (%) of the freeze-dried solids determined through pycnometer.

System	Degassed		Aerated	
	Freezing -40°C	Freezing cycles	Freezing -40°C	Freezing cycles
50% Coffee	34 ± 0.05	34 ± 0.02	33 ± 0.09	35 ± 0.33
60% Coffee	30 ± 0.36	35 ± 0.17	32 ± 0.07	30 ± 0.06
50% Gum arabic	35 ± 0.06	35 ± 0.08	24 ± 0.2	31 ± 0.04
60% Gum arabic	34 ± 0.07	26 ± 0.04	36 ± 0.05	25 ± 0.03

of the top layers of the solids were analysed and porosity was defined as the ratio between pore area and total area of the image (Silva et al., 2015). This method takes into account both open and closed pores, and results are shown in Table 3. Secondly, open porosity for each system was determined using a helium pycnometer (Chang, 1988). For these measurements, samples were taken by cutting throughout the cakes' heights, and results are shown in Table 4.

Although the two techniques are not directly comparable, as they refer to different sections of the cakes (i.e. the top layer was image-analysed, whereas both top and bottom layers were considered in pycnometer), overall the total porosities (Table 3) were higher than the open porosities (Table 4), indicating the presence of closed pores. In particular, similar open porosities (of the order of 25–35%) were observed for all systems, albeit with a trend for lower porosities at 60% initial solid concentration samples, compared to 50%.

Temperature oscillations during freezing resulted in higher total porosities by average 18% in both coffee and gum arabic, while the most affected morphologies were those of the aerated gum arabic systems. This observation agrees qualitatively with Fig. 6. Concentration also had an effect on total porosity, with dried 50% concentration systems showing higher porosities (by an average of 20%) than the dried 60% concentration systems, as also indicated qualitatively in Figs. 6 and 7. This excludes the 60% coffee frozen at -40°C , which showed high degree of puffing during freeze-drying making it difficult to sample from the top layer. Increased porosity

at 50% results from higher degree of water availability and crystallisation levels, compared to 60%, systems, which has also been linked with larger pore sizes in section 3.2.

Total porosities of aerated systems, compared to degassed, were higher for coffee (by 30% on average) and lower for gum arabic (by 7% on average). This may be linked with the phase separation observed in the freeze-dried aerated gum arabic systems, as air bubbles travelled to the top of the cake during freezing (see also section 3.2). The air bubble movement may have disrupted water crystallisation and hence led to lower total porosities of aerated gum arabic systems. For non-aerated systems, gum arabic showed higher total porosities than coffee. For these systems, Tables 1 and 2 indicate that it is easier for water to crystallise in gum arabic than coffee (higher freezing temperatures), and this may be linked with the higher porosities observed.

3.6. Reconstitution behavior of freeze-dried solids

Reconstitution kinetics of the freeze-dried solids are shown in Fig. 9 as area reduction of the solid particles over time. Overall, coffee samples dissolved approx. 8 times faster than gum arabic systems. Closer look of the dissolution images (see example snapshots of Fig. 10) indicated different reconstitution mechanisms for the two materials. Shortly after immersion in water, coffee particles disintegrated into small fragments that significantly increased the surface area of the material and resulted in fast reconstitution rates. By contrast, gum arabic particles dissolved from the outer surface to

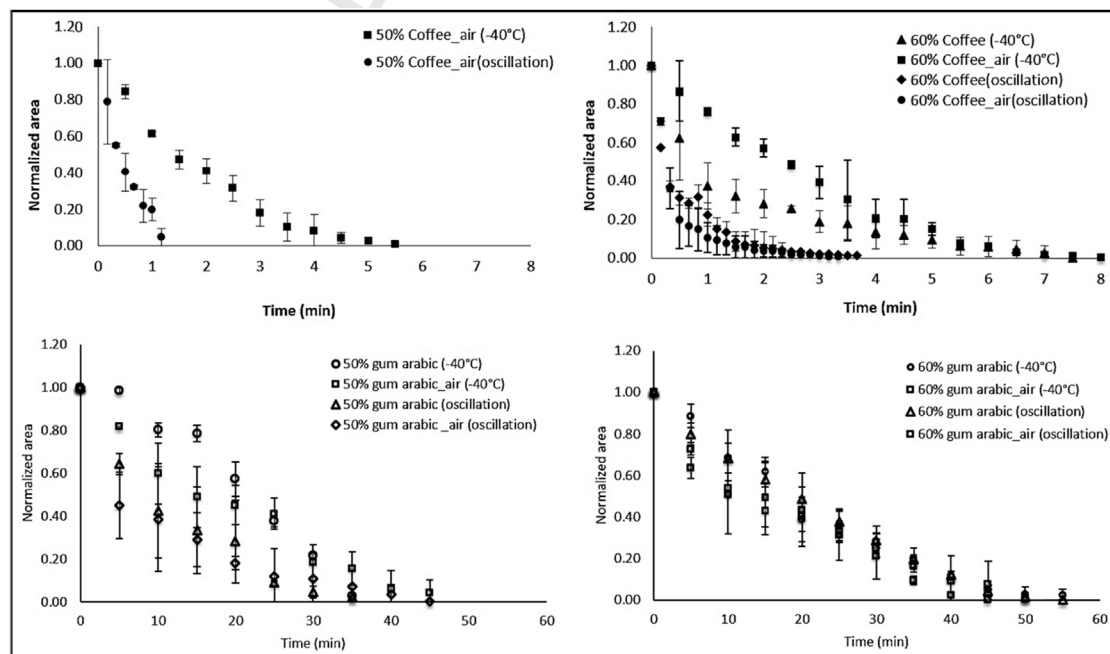


Fig. 9. Area reduction during dissolution of freeze-dried coffee and gum arabic affected by different formulation and freezing conditions.

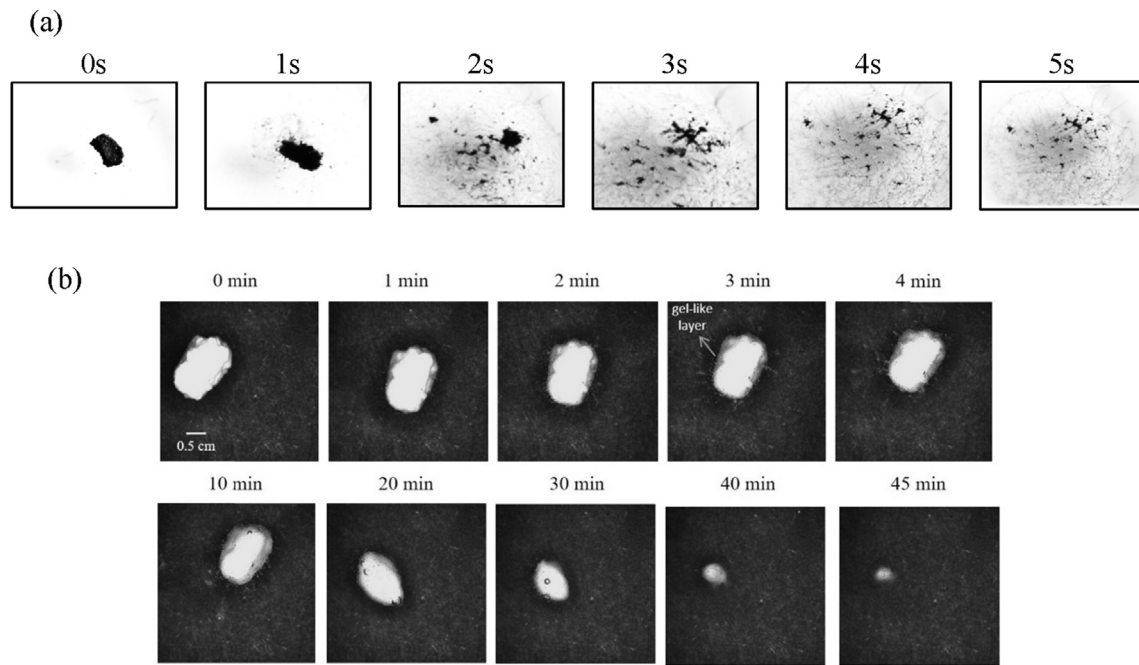


Fig. 10. Snapshots from dissolution tests performed on aerated and oscillated 60% systems: a) coffee; b) gum arabic.

the centre, after an apparent initial step of water absorption. This first step may have led to the formation of a gel-like layer that surrounds the particle and slows down dissolution (Kravtchenko et al., 1999; Miller-Chou & Koenig, 2003). In the images of Fig. 10, visible changes in the particle area of the gum arabic system are evident 10min after immersion into water.

Reconstitution kinetics appeared to correlate well with the microstructural data of section 3. Overall, systems with wider dendrite network and higher total estimated porosities showed faster reconstitution rates. As such, reconstitution was faster for the

50% systems, compared to the 60% systems, with complete reconstitution happening 2–3 min earlier (or approx. 40% faster) for coffee and 10min earlier (or approx. 25% faster) for gum arabic. Further, freezing cycles, again associated with wider dendrite network and increased porosities, resulted in higher reconstitution rates. Zea et al. (2013) and Saifullah et al. (2016) reported similar findings on the effect of porosity with fruit tablets prepared from freeze-dried powder. Previous works on the effect of pore size on rehydration kinetics have indicated that small pores result in slower rehydration in freeze-dried rice (Koh et al., 2011) but faster

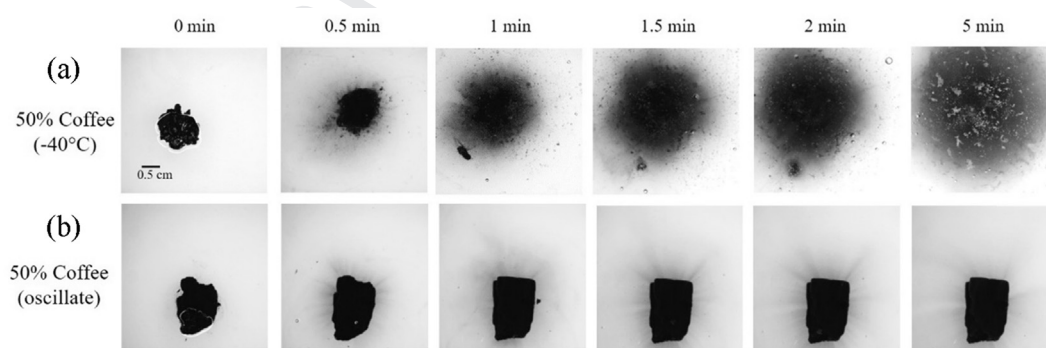


Fig. 11. Snapshots from dissolution of 50% coffee subjected to different freezing conditions.

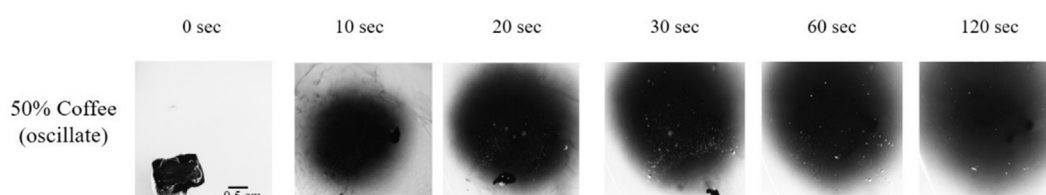


Fig. 12. Snapshots from dissolution of 50% coffee (oscillated) in hot distilled water (90°C).

rehydration in freeze-dried soy bean curd (Harnkarnsujarit et al., 2016). It appears that the mechanism of hydration, such as the relative importance of capillary imbibition and diffusion, largely determines the link between porosity and reconstitution kinetics (Harnkarnsujarit et al., 2016; Meda & Ratti, 2005; Saguy, Marabi, & Wallach, 2005).

An interesting case is that of the puffed 60% coffee frozen at -40°C , which rehydrated faster than the aerated system. In this sample, initial reconstitution rate was fast, which is linked with the highly porous structure of the puffed lower layer of the material. It appears that after dissolution of the puffed part of the solid, reconstitution of the top layer was significantly slower, and comparable to the 60% aerated system frozen at -40°C .

Notably, reconstitution of degassed 50% coffee systems is not shown in Fig. 9. For the system frozen at -40°C , determination of the reduction in the particle area was difficult due to rapid cloud formation on immersion in water (see Fig. 11a). For the system frozen with freezing cycles, the particle remained undissolved (see Fig. 11b), which was surprising. However, when dissolution for this particular sample was carried out at higher water temperature (90°C) it dissolved in under 5 min, forming a cloud similar to that formed during reconstitution of the 50% coffee frozen at -40°C (see Fig. 12).

4. Conclusion

This work demonstrates the potential to manipulate the properties (microstructure and reconstitution capacity) of freeze-dried highly concentrated (50 & 60% w/w) hydrocolloid-based systems by controlling the formulation and freezing conditions. This is important for applications targeted to produce freeze-dried materials with desired characteristics at lower energy and water use.

Concentration, aeration, and temperature fluctuations (at temperatures $< T_m$) during freezing all had an effect on determining the material's characteristics. Overall, lower concentration, aeration, and freezing temperature cycles were associated with larger pores, higher total porosities, and faster reconstitution rates. However, puffing of the material during drying resulted in microstructural changes and associated rehydration properties. For example, at

60% coffee frozen at -40°C , the degassed system rehydrated faster than the aerated, contrary to general observations. It was further observed that the two investigated materials (coffee & gum arabic) showed different reconstitution mechanisms, resulting in different reconstitution rates, with the coffee samples rehydrating faster than the gum arabic systems.

These findings support a strong link between formulation, freezing conditions, and properties of the dried material, further opening up opportunities for the design of energy efficient freeze-drying cycles without compromising product quality.

Uncited References

Wang and Martynenko, 2016; Harnkarnsujarit et al., 2016

References

Arvanitoyannis, I., et al. (1993). Calorimetric study of the glass transition occurring in fructose solutions. *Journal of the Science of Food and Agriculture*, 63, 177–188.

Asami, D. K., et al. (2003). Comparison of the total phenolic and ascorbic acid content of freeze-dried and air-dried marionberry, strawberry, and corn grown using conventional, organic, and sustainable agricultural practices. *Journal of Agricultural and Food Chemistry*, 51, 1237–1241.

Barresi, A. A., et al. (2009). Freeze drying of pharmaceutical excipients close to collapse Temperature: Influence of the process conditions on process time and product quality. *Drying Technology*, 27(6), 805–816.

Burmester, K., Fehr, H., & Eggers, R. (2011). A comprehensive study on thermo-physical material properties for an innovative coffee drying process. *Drying*

Technology, 29(February 2015), 1562–1570.

Capek, P., et al. (2010). Structural features of an arabinogalactan-protein isolated from instant coffee powder of *Coffea arabica* beans. *Carbohydrate Polymers*, 80(1), 180–185.

Cassanelli, M., Norton, I., & Mills, T. (2017). Role of gellan gum microstructure in freeze drying and rehydration mechanisms. *Food Hydrocolloids*, 75, 51–61.

Ceballos, A. M., Giraldo, G. I., & Orrego, C. E. (2012). Effect of freezing rate on quality parameters of freeze dried soursop fruit pulp. *Journal of Food Engineering*, 111(2), 360–365.

Chang, C. S. (1988). Measuring density and porosity of grain kernels using a gas pycnometer. *Cereal Chemistry*, 65(1), 13–15.

Franks, F. (1998). Freeze-drying of bioproducts: Putting principles into practice. *European Journal of Pharmaceutics and Biopharmaceutics*, 45(3), 221–229.

Gashua, I. B., Williams, P. A., & Baldwin, T. C. (2016). Molecular characteristics, association and interfacial properties of gum Arabic harvested from both *Acacia Senegal* and *Acacia seyal*. *Food Hydrocolloids*, 61, 514–522.

Gormley, R., et al. (2002). The effect of fluctuating vs. Constant frozen storage temperature regimes on some quality parameters of selected food products. *Lebensmittel-Wissenschaft und -Technologie- Food Science and Technology*, 35(2), 190–200. Available at: <http://www.sciencedirect.com/science/article/pii/S0023643801908370>.

Harnkarnsujarit, N., Charoenrein, S., & Roos, Y. H. (2012). Microstructure formation of maltodextrin and sugar matrices in freeze-dried systems. *Carbohydrate Polymers*, 88(2), 734–742.

Harnkarnsujarit, N., et al. (2016). Effects of freezing on microstructure and rehydration properties of freeze-dried soybean curd. *Journal of Food Engineering*, 184, 10–20.

Harnkarnsujarit, N., Kawai, K., & Suzuki, T. (2016). Impacts of freezing and molecular size on structure, mechanical properties and recrystallization of freeze-thawed polysaccharide gels. *Lebensmittel-Wissenschaft und -Technologie- Food Science and Technology*, 68, 190–201.

Homer, S., Kelly, M., & Day, L. (2014). Determination of the thermo-mechanical properties in starch and starch/gluten systems at low moisture content - a comparison of DSC and TMA. *Carbohydrate Polymers*, 108(1), 1–9.

Hottot, A., Vessot, S., & Andrieu, J. (2004a). A direct characterization method of the ice morphology. Relationship between mean crystals size and primary drying times of freeze-drying processes. *Drying Technology*, 22(8), 2009–2021.

Hottot, A., Vessot, S., & Andrieu, J. (2004b). A direct characterization method of the ice morphology. Relationship between mean crystals size and primary drying times of freeze-drying processes. *Drying Technology*, 22(January 2015), 2009–2021.

Hottot, A., Vessot, S., & Andrieu, J. (2007). Freeze drying of pharmaceuticals in vials: Influence of freezing protocol and sample configuration on ice morphology and freeze-dried cake texture. *Chemical Engineering and Processing: Process Intensification*, 46(7), 666–674.

Huang, L., et al. (2009). Studies on decreasing energy consumption for a freeze-drying process of apple slices. *Drying Technology*, 27(9), 938–946.

Ishwarya, S. P., & Anandharamakrishnan, C. (2015). Spray-Freeze-Drying approach for soluble coffee processing and its effect on quality characteristics. *Journal of Food Engineering*, 149, 171–180.

Kasper, J. C., & Friess, W. (2011). The freezing step in lyophilization: Physico-chemical fundamentals, freezing methods and consequences on process performance and quality attributes of biopharmaceuticals. *European Journal of Pharmaceutics and Biopharmaceutics*, 78(2).

Kiani, H., & Sun, D. W. (2011). Water crystallization and its importance to freezing of foods: A review. *Trends in Food Science & Technology*, 22(8), 407–426.

Koh, S., Rhim, J. W., & Kim, J. M. (2011). Effect of freezing temperature on the rehydration properties of freeze-dried rice porridge. *Korean Journal of Food Science and Technology*, 43(4), 509–512.

Kravtchenko, T. P., et al. (1999). A novel method for determining the dissolution kinetics of hydrocolloid powders. *Food Hydrocolloids*, 13(3), 219–225.

Krokida, M. K., Karathanos, V. T., & Maroulis, Z. B. (1998). Effect of freeze-drying conditions on shrinkage and porosity of dehydrated agricultural products. *Journal of Food Engineering*, 35(4), 369–380.

Kudra, T., & Ratti, C. (2006). Foam-mat drying: Energy and cost analyses. *Canadian Biosystems Engineering/Le Genie des biosystems au Canada*, 48, 27–32.

Levi, G., & Karel, M. (1995). Volumetric shrinkage (collapse) in freeze-dried carbohydrates above their glass transition temperature. *Food Research International*, 28(2), 145–151.

Liapis, A. I., & Bruttini, R. (2008). Exergy analysis of freeze drying of pharmaceuticals in vials on trays. *International Journal of Heat and Mass Transfer*, 51(15–16), 3854–3868.

Liliana, S.-C., Diana, P. V.-M., & Alfredo, A. A. (2015). Structural, physical, functional and nutraceutical changes of freeze-dried fruit. *African Journal of Biotechnology*, 14(6), 442–450. Available at: <http://academicjournals.org/journal/AJB/article-abstract/B98D7FF50317>.

Li, J. M., & Nie, S. P. (2016). The functional and nutritional aspects of hydrocolloids in foods. *Food Hydrocolloids*, 53, 46–51.

Liu, Y., Zhao, Y., & Feng, X. (2008). Exergy analysis for a freeze-drying process. *Applied Thermal Engineering*, 28(7), 675–690.

Luo, R., & Zhou, G. (2008). Mathematical optimization for energy consumption during freeze-drying of cooked beef slice. *Journal of Food Process Engineering*, 31(5), 583–601.

Meda, L., & Ratti, C. (2005). Rehydration of freeze-dried strawberries at varying temperatures. *Journal of Food Process Engineering*, 28(3), 233–246.

- Miller-Chou, B. A., & Koenig, J. L. (2003). A review of polymer dissolution. *Progress in Polymer Science*, 28(8), 1223–1270.
- Moreno, F. L., et al. (2015). Rheological behaviour, freezing curve, and density of coffee solutions at temperatures close to freezing. *International Journal of Food Properties*, 18(March), 426–438.
- Muthukumar, A., Ratti, C., & Raghavan, V. (2008). Foam-mat freeze drying of egg white-mathematical modeling Part II: Freeze drying and modeling. *Drying Technology*, 26(4), 513–518.
- Nakagawa, K., et al. (2006). Influence of controlled nucleation by ultrasounds on ice morphology of frozen formulations for pharmaceutical proteins freeze-drying. *Chemical Engineering and Processing: Process Intensification*, 45, 783–791.
- Nishino, M., Katayama, T., Sakata, M., Al-Assaf, S., & Philip, G. O. (2011). Effect of AGP on emulsifying stability of gum Arabic. *Gum Arabic*.
- Nowak, D., et al. (2016). Impact of material structure on the course of freezing and freeze-drying and on the properties of dried substance, as exemplified by celery. *Journal of Food Engineering*, 180, 22–28.
- Nunes, F. M., & Coimbra, M. A. (2002). Chemical characterization of the high-molecular-weight material extracted with hot water from green and roasted robusta coffees as affected by the degree of roast. *Journal of Agricultural and Food Chemistry*, 50(24), 7046–7052.
- Nussinovitch, A., Velez-Silvestre, R., & Peleg, M. (1993). Compressive characteristics of freeze-dried agar and alginate gel sponges. *Biotechnology Progress*, 9(1), 101–104.
- Overcashier, D. E., Patapoff, T. W., & Hsu, C. C. (1999). Lyophilization of protein formulations in vials: Investigation of the relationship between resistance to vapor flow during primary drying and small-scale product collapse. *Journal of Pharmaceutical Sciences*, 88(7), 688–695.
- Pardo, J. M., & Leiva, D. A. (2010). *Effect of different pre-treatments on energy consumption during freeze drying of pineapple pieces* (Vol. 35, pp. 934–938).
- Pardo, J. M., Suess, E., & Niranjan, K. (2002). An investigation into the relationship between freezing rate and mean ice crystal size for coffee extracts. *Food and Bioprocess Processing*, 80(September), 176–182.
- Patel, S. M., Doen, T., & Pikal, M. J. (2010). Determination of end point of primary drying in freeze-drying process control. *AAPS PharmSciTech*, 11(1), 73–84.
- Patel, S. M., et al. (2017). Lyophilized drug product cake Appearance: What is acceptable? *Journal of Pharmaceutical Sciences*, 106(7), 1706–1721.
- Petzold, G., & Aguilera, J. M. (2009). Ice morphology: Fundamentals and technological applications in foods. *Food Biophysics*, 4(4), 378–396.
- Raharitsifa, N., & Ratti, C. (2010). Foam-mat freeze-drying of apple juice part 1: Experimental data and ann simulations. *Journal of Food Process Engineering*, 33, 268–283.
- Rahman, M. S. (2006). State diagram of foods: Its potential use in food processing and product stability. *Trends in Food Science & Technology*, 17(3), 129–141.
- Rambhatla, S., et al. (2004). Heat and mass transfer scale-up issues during freeze drying: II. Control and characterization of the degree of supercooling. *AAPS PharmSciTech*, 5(4), 1–9.
- Roos, Y. H. (1997). Frozen state transitions in relation to freeze drying. *Journal of Thermal Analysis*, 48, 535–544.
- Roos, Y. H., & Karel, M. (1991). Amorphous state and delayed ice formation in sucrose solutions. *International Journal of Food Science and Technology*, 26(6), 553–566.
- Saguy, I. S., Marabi, A., & Wallach, R. (2005). Liquid imbibition during rehydration of dry porous foods. *Innovative Food Science & Emerging Technologies*, 6(1), 37–43.
- Saifullah, M., et al. (2016). Physicochemical and flow properties of fruit powder and their effect on the dissolution of fast dissolving fruit powder tablets. *Powder Technology*, 301, 396–404. Available at: <https://doi.org/10.1016/j.powtec.2016.06.035>.
- Sangamithra, A., et al. (2015). Foam mat drying of food materials: A review. *Journal of Food Processing and Preservation*, 39(6), 3165–3174.
- Searles, J. A. (2010). Freeze drying/lyophilization of pharmaceutical and biological products. In L. Rey, & J. C. May (Eds.), *Freeze drying/lyophilization of pharmaceutical and biological products* (pp. 1–28). New York: Informa Healthcare.
- Searles, J. A., Carpenter, J. F., & Randolph, T. W. (2001). The ice nucleation temperature determines the primary drying rate of lyophilization for samples frozen on a temperature-controlled shelf. *Journal of Pharmaceutical Sciences*, 90(7), 860–871.
- Silva, J. V. C., et al. (2015). Characterization of the microstructure of dairy systems using automated image analysis. *Food Hydrocolloids*, 44, 360–371.
- Tsourouflis, S., Flink, J. M., & Karel, M. (1976). Loss of structure in freeze-dried carbohydrates solutions: Effect of temperature, moisture content and composition. *Journal of the Science of Food and Agriculture*, 27(6), 509–519.
- Ullrich, S., Seyferth, S., & Lee, G. (2015). Measurement of shrinkage and cracking in lyophilized amorphous cakes. Part II: Kinetics. *Pharmaceutical Research*, 32(8), 2503–2515.
- Voda, A., et al. (2012). The impact of freeze-drying on microstructure and rehydration properties of carrot. *Food Research International*, 49(2), 687–693.
- Wang, D., & Martynenko, A. (2016). Estimation of total, open-, and closed-pore porosity of apple slices during drying. *Drying Technology*, 34(8), 892–899.
- Xu, Y., et al. (2006). A two-stage vacuum freeze and convective air drying method for strawberries. *Drying Technology*, 24(February 2015), 1019–1023.
- Zea, L. P., et al. (2013). Compressibility and dissolution characteristics of mixed fruit tablets made from guava and pitaya fruit powders. *Powder Technology*, 247, 112–119.